

Oxidation of Dopamine in the Presence of Cysteine: Characterization of New Toxic Products

Xue-Ming Shen, Fa Zhang, and Glenn Dryhurst*

Department of Chemistry and Biochemistry, University of Oklahoma, Norman, Oklahoma 73019

Received August 15, 1996[⊗]

Previous studies demonstrated that oxidation of dopamine (DA) in the presence of L-cysteine (CySH) at pH 7.4 gives a complex mixture of cysteinyl conjugates of the neurotransmitter that can be easily further oxidized to a number of dihydrobenzothiazines (DHBTs) along with unidentified yellow products. In this investigation, three of these products have been identified. 7-(2-Aminoethyl)-5-hydroxy-1,4-benzothiazine-3-carboxylic acid (BT-1) is formed as a result of oxidation of 5-*S*-cysteinyl dopamine (5-*S*-CyS-DA) and 7-(2-aminoethyl)-3,4-dihydro-5-hydroxy-2*H*-1,4-benzothiazine-3-carboxylic acid (DHBT-1). Regioisomers 6-(2-aminoethyl)-1,8,9,10-tetrahydrobenzo[1,2-*b*:4,3-*b'*]bis[1,4]thiazine-9-carboxylic acid (**12**) and 6-(2-aminoethyl)-1,2,3,10-tetrahydrobenzo[1,2-*b*:4,3-*b'*]bis[1,4]thiazine-2-carboxylic acid (**13**) are formed by oxidation of 2,5-bi-*S*-cysteinyl dopamine (2,5-bi-*S*-CyS-DA), 6-*S*-cysteinyl-7-(2-aminoethyl)-3,4-dihydro-5-hydroxy-2*H*-1,4-benzothiazine-3-carboxylic acid (DHBT-2), and 6-*S*-cysteinyl-8-(2-aminoethyl)-3,4-dihydro-5-hydroxy-2*H*-1,4-benzothiazine-3-carboxylic acid (DHBT-6). 2,5-Bi-*S*-CyS-DA, DHBT-2, and DHBT-6 are major early products of DA oxidation in the presence of CySH. However, because these three compounds are the most easily oxidized products formed in this reaction, they are subsequently transformed into **12** and **13**, the latter regioisomer always being the major product. Both **12** (LD₅₀ = 18.5 μg) and **13** (LD₅₀ = 1.5 μg) are lethal when administered into the brains of mice and evoke hyperactivity and tremor. The potential relevance of the in vitro chemistry described in this and earlier reports to reactions that might occur in neuromelanin-pigmented dopaminergic neurons in Parkinson's disease is discussed.

Introduction

Recent reports from this laboratory have described the influence of L-cysteine (CySH)¹ on the in vitro oxidation chemistry of the catecholaminergic neurotransmitter dopamine (DA) at neutral pH (1–3). These studies have demonstrated that CySH diverts the normal oxidation of DA to dark brown/black melanin polymer (4, 5) by scavenging the proximate oxidation product of the neurotransmitter, DA-*o*-quinone (**1**), to form initially 5-*S*-

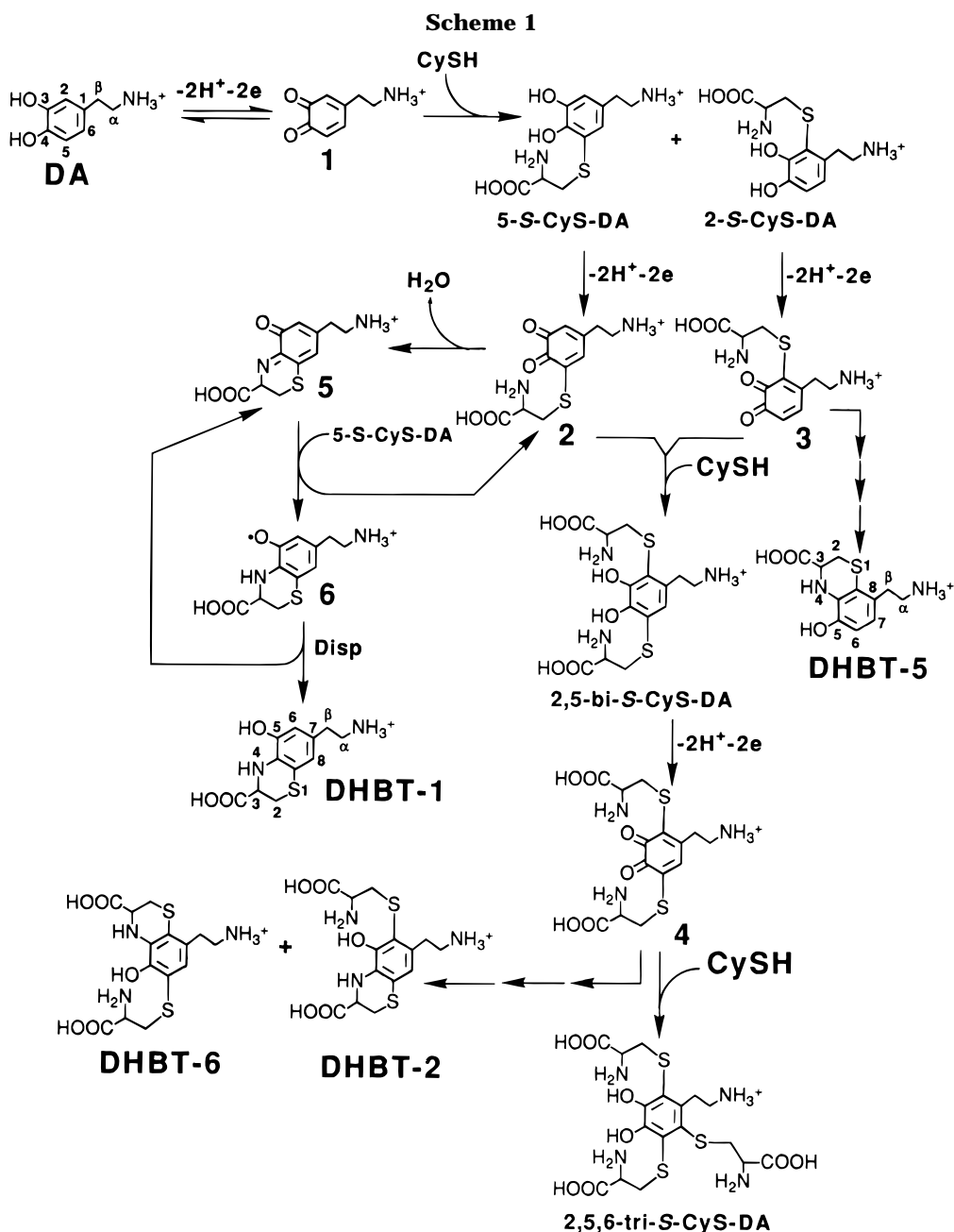
cysteinyl dopamine (5-*S*-CyS-DA; major product) and 2-*S*-cysteinyl dopamine (2-*S*-CyS-DA; minor product) (Scheme 1). Both 5-*S*- and 2-*S*-CyS-DA are more easily oxidized than DA (1, 2). Thus, under conditions where DA is oxidized, these cysteinyl conjugates are also further oxidized. In the presence of free CySH, the in vitro oxidations of 5-*S*-CyS-DA and 2-*S*-CyS-DA follow several pathways, one of which leads to 2,5-bi-*S*-cysteinyl dopamine (2,5-bi-*S*-CyS-DA) and thence 2,5,6-tri-*S*-cysteinyl dopamine (2,5,6-tri-*S*-CyS-DA) by the pathways shown in Scheme 1. However, *o*-quinones such as **2** and **3**, proximate oxidation products of 5-*S*-CyS-DA and 2-*S*-CyS-DA, respectively, can also undergo intramolecular cyclization reactions (1–3). To illustrate, intramolecular cyclization of **2** yields *o*-quinone imine **5** that can chemically oxidize 5-*S*-CyS-DA to **2** with concomitant formation of radical **6**. Disproportionation of **6** then gives dihydrobenzothiazine (DHBT)-1² and **5**. Similar reaction pathways lead to DHBT-5 from 2-*S*-CyS-DA and DHBT-2 and DHBT-6 from 2,5-bi-*S*-CyS-DA (Scheme 1) (2). Details of the reaction pathways leading to these and other DHBTs have been presented elsewhere (2). However, not only are most cysteinyl conjugates of DA more easily oxidized than the neurotransmitter but so also are the resulting DHBTs. In our earlier investigations it was noted that oxidations of DA in the presence of free CySH gave, in addition to cysteinyl dopamines and DHBTs, additional bright yellow products. Formation of these

* Address correspondence to this author: Tel (405) 325-4811; Fax (405) 325-6111; E-mail gdryhurst@chemdept.chem.uoknor.edu.

[⊗] Abstract published in *Advance ACS Abstracts*, January 1, 1997.

¹ Abbreviations: Parkinson's disease, PD; substantia nigra, SN; dopamine, DA; dopamine-*o*-quinone, **1**; L-cysteine, CySH; glutathione, GSH; glutathione disulfide, GSSG; 5-*S*-cysteinyl dopamine, 5-*S*-CyS-DA; homovanillic acid, HVA; cerebrospinal fluid, CSF; γ -glutamyl transpeptidase, γ -GT; 2-*S*-cysteinyl dopamine, 2-*S*-CyS-DA; 2,5-bi-*S*-cysteinyl dopamine, 2,5-bi-*S*-CyS-DA; 2,5,6-tri-*S*-cysteinyl dopamine, 2,5,6-tri-*S*-CyS-DA; dihydrobenzothiazine, DHBT; 7-(2-aminoethyl)-3,4-dihydro-5-hydroxy-2*H*-1,4-benzothiazine-3-carboxylic acid, DHBT-1; 6-*S*-cysteinyl-7-(2-aminoethyl)-3,4-dihydro-5-hydroxy-2*H*-1,4-benzothiazine-3-carboxylic acid, DHBT-2; 6-*S*-cysteinyl-8-(2-aminoethyl)-3,4-dihydro-5-hydroxy-2*H*-1,4-benzothiazine-3-carboxylic acid, DHBT-6; pyrolytic graphite electrode, PGE; saturated calomel reference electrode, SCE; nuclear magnetic resonance, NMR; fast atom bombardment mass spectrometry, FAB-MS; high-performance liquid chromatography, HPLC; 7-(2-aminoethyl)-5-hydroxy-1,4-benzothiazine-3-carboxylic acid, BT-1; retention time, *t*_R; trifluoroacetic acid, TFA; 6-(2-aminoethyl)-1,8,9,10-tetrahydrobenzo[1,2-*b*:4,3-*b'*]bis[1,4]thiazine-9-carboxylic acid, **12**; 6-(2-aminoethyl)-1,2,3,10-tetrahydrobenzo[1,2-*b*:4,3-*b'*]bis[1,4]thiazine-2-carboxylic acid, **13**; 6-(2-aminoethyl)-1,2,3,8,9,10-hexahydrobenzo[1,2-*b*:4,3-*b'*]bis[1,4]thiazine-9-carboxylic acid, **14**; 6-(2-aminoethyl)-1,2,3,8,9,10-hexahydrobenzo[1,2-*b*:4,3-*b'*]bis[1,4]thiazine-2-carboxylic acid, **15**; heteronuclear multiple-quantum coherence, HMQC; heteronuclear multiple bond connectivity, HMBC; peak potential, *E*_p; dimethyl sulfoxide, Me₂SO.

² Abbreviations used for various dihydrobenzothiazines (DHBTs) are identical to those employed in an earlier paper (2).



yellow products was favored by long oxidation times or when DA was oxidized in the presence of relatively low concentrations of CySH. This suggested that these products are formed by oxidation of one or more DHBTs or by alternative oxidative pathways from cysteinyl-dopamine precursors. However, we were unable to isolate and identify any of these yellow secondary products in our earlier investigation.

Our interest in investigating the influence of CySH on the oxidation chemistry of DA stems from a number of lines of evidence that have led us to propose that similar reactions might occur in neuromelanin-pigmented dopaminergic neurons in the substantia nigra (SN) pars compacta in Parkinson's disease (PD). Dopaminergic SN cells are pigmented with black neuromelanin as a result of the autoxidation of cytoplasmic DA to **1** that oxidatively polymerizes (6, 7). Similar to other neuronal cell bodies, dopaminergic SN neurons normally contain little or no CySH or glutathione (GSH) (8, 9). However, it has been reported that γ -glutamyl transpeptidase (γ -GT) is significantly upregulated in the Parkinsonian SN (10).

γ -GT is the only known mammalian enzyme that can cleave the γ -glutamyl bond of GSH to give CySH (11) and plays a key role in the translocation of CySH and hence GSH into cells, including neurons (12). Based, in part, on such factors we have proposed (1, 2) that a very early event in the pathogenesis of PD might be the γ -GT-mediated translocation of CySH, biosynthesized and exported along with GSH by nigral glial cells (13, 14), into neuromelanin-pigmented SN neurons (1, 2). Such a γ -GT-mediated translocation of CySH into these cells might account not only for the decreased neuromelanin content of surviving pigmented SN neurons (15–17) by scavenging *o*-quinone **1** but also for the irreversible loss of nigral GSH that is not accompanied by a corresponding increase of glutathione disulfide (GSSG) (18–20), the increased 5-*S*-CyS-DA/DA concentration ratio in the SN (21), and the increased 5-*S*-CyS-DA/homovanillic acid (HVA) ratio in cerebrospinal fluid (CSF) (22), all of which occur in PD. Furthermore, we have also speculated that one or more of the metabolites that should be formed in the cytoplasm of SN cells as a consequence of the CySH-

mediated diversion of the neuromelanin pathways might include endotoxins that contribute to the selective degeneration of nigrostriatal dopaminergic neurons in PD. Whether any cysteinyl dopamines or DHBTs are indeed dopaminergic neurotoxins remains to be established although 2,5-bi-*S*-CyS-DA and several DHBTs are toxic (lethal) when administered into the brains of mice (1, 2). However, the various cysteinyl conjugates of DA and resultant DHBTs discovered in our previous investigations represent the products formed in the early stages of oxidation of the neurotransmitter in the presence of CySH. These putative nigral metabolites are more easily oxidized than DA at physiological pH and, hence, if formed in the cytoplasm of SN neurons would be expected to undergo further oxidation reactions. Accordingly, the principal goal of the present investigations was to identify the major products responsible for the bright yellow color that develops as a result of more prolonged oxidation of DA in the presence of CySH. As in previous investigations (1–3), electrochemical methods have been employed to generate *o*-quinone **1** from DA. Because **1** is formed as a result of chemical (6, 7), enzymatic (9), and electrochemical (1–5) oxidations of DA, it was judged reasonable to expect that the results of this and earlier studies are probably relevant to the chemistry that is speculated to occur in the cytoplasm of SN neurons in PD.

Materials and Methods

Caution. Compound **12** and particularly compound **13**, in addition to 2,5-bi-*S*-CyS-DA, DHBT-1, DHBT-2, and DHBT-6, are lethal when administered into the brains of mice and, hence, should be regarded as potentially hazardous to humans and therefore handled with care. Such chemicals should always be handled with protective gloves and in a hood.

Chemicals. Dopamine hydrochloride (DA-HCl) and L-cysteine (CySH) were obtained from Sigma (St. Louis, MO). HPLC grade acetonitrile (MeCN) was obtained from EM Science (Gibbstown, NJ). Concentrated trifluoroacetic acid (TFA) was obtained from Aldrich (Milwaukee, WI). 2,5-Bi-*S*-cysteinyl-dopamine (2,5-bi-*S*-CyS-DA), 7-(2-aminoethyl)-3,4-dihydro-5-hydroxy-2*H*-1,4-benzothiazine-3-carboxylic acid (DHBT-1), 6-*S*-cysteinyl-7-(2-aminoethyl)-3,4-dihydro-5-hydroxy-2*H*-1,4-benzothiazine-3-carboxylic acid (DHBT-2), and 6-*S*-cysteinyl-8-(2-aminoethyl)-3,4-dihydro-5-hydroxy-2*H*-1,4-benzothiazine-3-carboxylic acid (DHBT-6) were electrochemically synthesized, isolated, and purified as described previously (2).

Electrochemistry. Voltammograms were obtained at a pyrolytic graphite microelectrode (PGE; Pfizer Minerals, Pigments and Metals Division, Easton, PA) having an approximate surface area of 6 mm² as described previously (1–3). A conventional three-electrode voltammetric cell was used with a platinum wire counter electrode and a saturated calomel reference electrode (SCE). Cyclic voltammetry was carried out with a BAS-100A (Bioanalytical Systems, West Lafayette, IN) electrochemical analyzer. Controlled-potential electrolyses employed a Princeton Applied Research Corp. (Princeton, NJ) Model 173 potentiostat. A three-compartment cell was used in which the working, counter, and reference electrode compartments were separated with a Nafion membrane (type 117, DuPont Co., Wilmington, DE). The working electrode consisted of several plates of pyrolytic graphite having a total surface area of ~180 cm². The counter electrode was platinum gauze, and a SCE reference electrode was used. The solution in the working electrode compartment was vigorously bubbled with N₂ and stirred with a Teflon-coated magnetic stirring bar. All potentials are referenced to the SCE at ambient temperature (22 ± 2 °C).

Spectroscopy. NMR spectra were recorded on either a Varian (Palo Alto, CA) XL-300 or VXR-500 spectrometer. Low- and high-resolution fast atom bombardment mass spectrometry

(FAB-MS) employed a VG Instruments (Manchester, U.K.) ZAB-E spectrometer. Thermospray mass spectra were obtained with a Kratos (Manchester, U.K.) MS25/RFA spectrometer equipped with a thermospray source. UV-visible spectra were recorded on a Hewlett-Packard (Palo Alto, CA) Model 8452A diode array spectrophotometer.

High-Performance Liquid Chromatography. HPLC employed two Gilson (Middleton, WI) gradient systems equipped with either dual Model 302 pumps (10 mL pump heads) or dual Model 306 pumps (25 mL pump heads). Both systems were computer-controlled and were equipped with Rheodyne (Cotati, CA) Model 7125 injectors and UV detectors set at 254 nm. Preparative-scale, reversed phase columns (Bakerbond C₁₈, 10 μm, 250 × 21.2 mm) were used. Four mobile phase solvents were employed for HPLC. Solvent A was deionized water. Solvent B was a 1:1 solution of MeCN and deionized water. Solvent C was prepared by adding concentrated TFA to deionized water until the pH was 2.15. Solvent D was prepared by adding TFA to a 1:1 solution of MeCN and deionized water until the pH was 2.15.

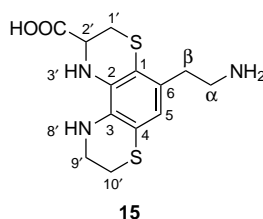
HPLC method I employed solvents A and B and the following gradient: 0–10 min, 100% solvent A; 10–98 min, linear gradient to 24% solvent B; 98–101 min, linear gradient to 100% solvent B; 101–113 min, 100% solvent B. The flow rate was constant at 7 mL min⁻¹.

HPLC method II employed solvents C and D and the following gradient: 0–97 min, linear gradient from 100% solvent C to 38% solvent D; 97–100 min, linear gradient to 100% solvent D; 100–113 min, 100% solvent D. The flow rate was constant at 7 mL min⁻¹.

Oxidation Reaction Procedure. DA-HCl (5.7 mg; 1.0 mM) and CySH (1.82–7.28 mg; 0.5–2.0 mM) were dissolved in 30 mL of phosphate buffer (pH 7.4; μ = 0.2) and the resulting solution was electrolyzed at 50–100 mV for 60 min. Upon termination of the reaction, the entire volume of the yellow product solution was pumped onto the reversed phase column and reactants and products were separated using HPLC method I. The solutions eluted under the chromatographic peaks corresponding to major products were collected separately and immediately frozen at –80 °C (dry ice). Following several repetitive experiments, the combined solutions containing each product was purified several times using HPLC method I. The resulting solutions containing purified products were then freeze-dried.

Spectroscopic and chemical evidence in support of the proposed structures of products is presented below. Complete chemical names are provided for each new compound. However, for simplicity, the slightly modified atom numbering systems for **12**–**15** shown in Scheme 2 and Table 1 are employed to assign resonances in ¹H and ¹³C NMR spectra. The purity of each new compound (**12**–**15**) was estimated to be ≥99% on the basis of analytical HPLC using a reversed phase systems and both UV (254 nm) and electrochemical (0.80 V vs Ag/AgCl; glassy carbon detector electrode) detectors.

7-(2-Aminoethyl)-5-hydroxy-1,4-benzothiazine-3-carboxylic Acid (BT-1). In the HPLC mobile phase (method I; ~6% MeCN in water), BT-1 gave a bright yellow solution (λ_{max} = 342, ~300 shoulder (sh), 246, 216 nm). The thermospray mass spectrum of this solution gave *m/z* = 253 (MH⁺, 100%). A comparison of these spectral data and the cyclic voltammetric behavior of BT-1 with model compounds previously permitted a tentative structure for this benzothiazine to be assigned (3). However, efforts to isolate BT-1 and to obtain spectroscopic evidence (NMR, FAB-MS) to directly confirm this structure were unsuccessful owing to the instability of this compound. However, similar structures have been elucidated as a result of borohydride reduction of benzothiazines to the corresponding dihydrobenzothiazines that can be isolated (23). Accordingly, a vigorously stirred solution of freshly chromatographed BT-1 dissolved in the HPLC mobile phase (method I) was treated with sodium borohydride as described elsewhere (23). During addition of NaBH₄ the bright yellow color of BT-1 disappeared to give a colorless solution. After 10 min, the solution (pH 7–8)

Table 1. ^1H (500 MHz), ^{13}C (125 MHz), HMQC, and HMBC Chemical Shift Assignments (ppm) for **15** and Carbons to Which Long-Range Connectivity Is Observed in HMBC Experiment^a

assignment	^1H (J in Hz)	^{13}C	HMQC (^{13}C)	HMBC (^{13}C)
β	2.80 (t, 7.5, 2H)	29.68	29.68	131.88 (C-6), 118.12 (C-5), 112.97 (C-1), 38.00 (C- α)
1'	3.03 (dd, 13.0, 3.5, 1H)	24.86	24.86	174.54 (COOH), 112.97 (C-1), 52.58 (C-2')
α	3.09 (t, 7.5, 2H)	38.00	38.00	131.88 (C-6), 29.68 (C- β)
10'	3.14 (m, 2H)	22.33	22.33	121.86 (C-4), 42.53 (C-9')
1'	3.25 (dd, 13.0, 4.5, 1H)	24.86	24.86	112.97 (C-1), 52.58 (C-2')
9'	3.67 (m, 2H)	42.53	42.53	117.13 (C-3), 22.33 (C-10')
2'	4.57 (dd, 4.5, 3.5, 1H)	52.58	52.58	174.54 (C=O), 133.533 (C-2)
5	6.51 (s, 1H)	118.12	118.12	117.13 (C-3), 112.97 (C-1), 29.68 (C- β)
6		131.88		
1		112.97		
2		133.53		
3		117.13		
4		121.86		
COOH		174.54		

^a **15** was dissolved in D_2O for all experiments.

preparative reversed phase column. Using HPLC method II, the reduced form of **12**, i.e., **14**, eluted at $t_R = 87$ min. In the HPLC mobile phase (pH 2.15) **14** exhibited a spectrum with $\lambda_{\text{max}} = 324, 284$ sh, 252 nm. The eluent containing **14** was freeze-dried to give a very pale yellow solid. In phosphate buffer (pH 7.4), **14** exhibited a UV spectrum at λ_{max} ($\log \epsilon_{\text{max}}, \text{M}^{-1} \text{cm}^{-1}$) 318 (3.37), 286 sh (3.82), and 256 (4.40) nm, calculated as the 2TFA salt (**2**). FAB-MS (3-nitrobenzyl alcohol matrix) gave $m/z = 312.0846$ (MH^+ , 40%, $\text{C}_{13}\text{H}_{18}\text{N}_3\text{O}_2\text{S}_2$; calcd $m/z = 312.0840$). ^1H NMR (300 MHz; D_2O) gave δ 6.59 (s, 1H, C(5)H), 4.54 (dd, $J = 4.8, 3.0$ Hz, 1H, C(9')H), 3.60–3.55 (m, 2H, C(2')H₂), 3.22 (dd, $J = 13.2, 4.8$ Hz, 1H, C(10')H), 3.18–3.10 (m, 3H, C(10')H, C(α)H₂), 3.08–3.04 (m, 2H, C(1')H₂), 2.87–2.80 (m, 2H, C(β)H₂). The assignment of ^1H resonances were confirmed by homonuclear decoupling and 2D COSY experiments. These spectral data were interpreted to indicate that **14** is 6-(2-aminoethyl)-1,2,3,8,9,10-hexahydrobenzo[1,2-*b*:4,3-*b'*]bis[1,4]thiazine-9-carboxylic acid formed by borohydride reduction of the C(2')=N(3') double bond of **12** (see later discussion).

6-(2-Aminoethyl)-1,2,3,10-tetrahydrobenzo[1,2-*b*:4,3-*b'*]bis[1,4]thiazine-2-carboxylic Acid (13**).** Compound **13** was isolated as a yellow solid. In phosphate buffer (pH 7.4), **13** exhibited a UV-visible spectrum with λ_{max} ($\log \epsilon_{\text{max}}, \text{M}^{-1} \text{cm}^{-1}$) at 386 (3.35), 332 (3.30), 290 sh (3.64), 264 sh (4.06), and 242 (4.22) nm. The thermospray mass spectrum of a solution of **13** dissolved in the HPLC mobile phase (method I) gave $m/z = 310$ (MH^+ , 100%). FAB-MS (thioglycerol/glycerol matrix) gave $m/z = 310.0711$ (MH^+ , 6%, $\text{C}_{13}\text{H}_{16}\text{N}_3\text{O}_2\text{S}_2$; calcd $m/z = 310.0684$). ^1H NMR (300 MHz; D_2O) gave δ 7.83 (t, $J = 4.2$ Hz, 1H, C(9')H), 6.54 (s, 1H, C(5)H), 4.27 (dd, $J = 5.4, 3.9$ Hz, 1H, C(2')H), 3.21–3.11 (m, 6H, C(1')H₂, C(10')H₂, C(α)H₂), 2.96–2.84 (m, 2H, C(β)H₂). The low solubility of **13** in D_2O (and all other common deuterated solvents) resulted in a very weak spectrum which precluded more extensive NMR studies. Additional evidence for the proposed structure of **13** was obtained by reducing a solution of this yellow compound dissolved in the HPLC method I mobile phase with NaBH_4 as described for **12** (**23**). The resulting colorless solution (pH 7–8) was adjusted to pH 2.15 with TFA and then pumped onto the preparative reversed phase column. Using HPLC method II, the reduced form of **13**, i.e., **15**, eluted at $t_R = 85$ min. In the HPLC mobile phase (pH 2.15) **15** exhibited a UV spectrum with $\lambda_{\text{max}} = 322, 282$ sh, and 250 nm. This solution was freeze-dried to give a very pale yellow solid. In phosphate buffer (pH 7.4) **15** exhibited a UV spectrum, λ_{max} ($\log \epsilon_{\text{max}}, \text{M}^{-1} \text{cm}^{-1}$) at 318 (3.32), 284 sh (3.82), and 254 (4.40) nm, calculated as the 2TFA salt (**2**). FAB-MS (3-

nitrobenzyl alcohol matrix) gave $m/z = 312.0833$ (MH^+ , 100%, $\text{C}_{13}\text{H}_{18}\text{N}_3\text{O}_2\text{S}_2$; calcd $m/z = 312.0840$). ^1H NMR (300 MHz; D_2O) gave δ 6.52 (s, 1H, C(5)H), 4.57 (dd, $J = 4.8, 3.0$ Hz, 1H, C(2')H), 3.63–3.59 (m, 2H, C(9')H₂), 3.28 (dd, $J = 13.2, 4.8$ Hz, 1H, C(1')H), 3.18–3.06 (m, 5H, C(10')H, C(10')H₂, C(α)H₂), 2.89–2.82 (m, 2H, C(β)H₂). These spectral data suggested that **15** was 6-(2-aminoethyl)-1,2,3,8,9,10-hexahydrobenzo[1,2-*b*:4,3-*b'*]bis[1,4]thiazine-2-carboxylic acid. Further evidence to support the proposed structure of **15** and hence **13** will be presented subsequently.

Animals. Outbred Adult Male Mice of the HSD:ICR albino strain (Harlan Sprague-Dawley, Madison, WI) weighing 32 ± 5 g were employed. Animals were housed 10 per cage, allowed free access to Purina rat chow and water, and maintained on a 12 h light/dark cycle with lights on a 7:00 a.m. Experimental mice were treated with test compounds dissolved in either 5 μL of isotonic saline (0.9% NaCl in deionized water) or 5 μL of 30% Me_2SO in aqueous isotonic saline. Prior to drug administration, animals were anesthetized with ether for 45–55 s. Injections were performed freehand with the point of puncture being 3 mm anterior to the interaural line, 1 mm left lateral of the midline, and 3 mm perpendicular to the scalp as described previously (**1**, **2**). Control animals were treated with 5 μL of vehicle alone under otherwise identical conditions. All animal procedures were approved by the Institutional Animal Care and Use Committee at the University of Oklahoma.

Results

Oxidation of DA in the Presence of CySH. A chromatogram (HPLC method I) of the product solution formed following controlled-potential electrooxidation of DA (1.0 mM) in the presence of CySH (1.0 mM) in phosphate buffer (pH 7.4; $\mu = 0.2$) at an applied potential of 50 mV for 60 min is shown in Figure 1A. Under these chromatographic conditions, cysteinyl-dopamines and most DHBTs formed in the reaction (described in detail elsewhere) (**1**, **2**) coeluted under the peaks at $t_R < 20$ min. However, four major products were well separated and, hence, could be isolated and spectroscopically identified: DHBT-1, BT-1, and regioisomers **12** and **13**. HPLC analysis (method I) of the product solution at earlier stages of the reaction (<60 min) revealed that the chromatographic peaks at $t_R < 20$ min and for DHBT-1

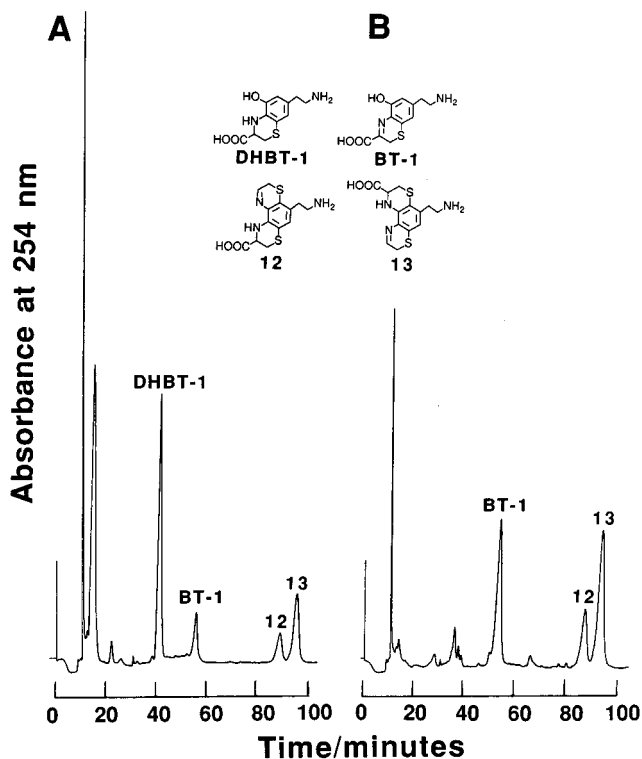


Figure 1. HPLC chromatograms (method I) of the product solutions formed following controlled-potential electrooxidation of DA (1.0 mM) and CySH (1.0 mM) in phosphate buffer (pH 7.4; $\mu = 0.2$) for 60 min at (A) 50 and (B) 100 mV.

($t_R = 39$ min) were significantly larger than those shown in Figure 1A. Correspondingly, peaks for BT-1, **12**, and **13** were smaller. These observations suggested that BT-1, **12**, and **13** were secondary products formed by further oxidation of cysteinyl-dopamines and/or DHBTs. Oxidation of DA (1.0 mM) in the presence of CySH (1.0 mM) in phosphate buffer (pH 7.4) for 60 min at a more positive applied potential (e.g., 100 mV) resulted in higher yields of BT-1, **12**, and **13** (Figure 1B). However, under these more strongly oxidizing conditions, DHBT-1 disappeared and the chromatographic peaks at $t_R < 20$ min decreased and disappeared. The yields of **12** and **13** were maximal when DA (1.0 mM) was oxidized in the presence of 2.0 mM CySH for 60 min at an applied potential of 100 mV. Under these conditions additional minor product peaks were observed in chromatograms of the reaction solution. In the presence of higher concentrations of CySH (≥ 3 mM), under otherwise identical conditions, the yields for these additional unidentified products increased. However, **12** and **13** remained as major reaction products. Controlled-potential electrooxidations of DA (1.0 mM) in the presence of CySH (0.5–5.0 mM) at potentials ranging from 0 to 100 mV always gave **12** and **13** as products. However, at low applied potentials (0 mV), very long electrolyses (> 120 min) were necessary before significant yields of BT-1, **12**, and **13** were observed. In view of the fact that BT-1, **12**, and **13** were formed under all conditions when DA (1.0 mM) was oxidized (0–100 mV) in the presence of CySH (0.5–5.0 mM) at pH 7.4, this investigation focused on the identification of these compounds.

In an earlier investigation (3), it was demonstrated that BT-1 is formed as a result of oxidation of both 5-*S*-CyS-DA and DHBT-1 at pH 7.4. However, attempts to isolate pure samples of BT-1 were unsuccessful owing to its decomposition particularly during the final freeze-

drying step. Based upon a comparison of the UV-visible spectrum, thermospray mass spectrum, and cyclic voltammetric behavior with those of more stable model compounds and the fact that it is formed as a result of oxidation of 5-*S*-CyS-DA and DHBT-1, a tentative structure for BT-1 was proposed in a previous study (3). This structure was confirmed on the basis that BT-1 could be reduced by NaBH₄ to the racemate of DHBT-1 (see Materials and Methods), a method employed by other investigators to elucidate the structure of similar benzothiazines (23).

Precursors of and Chemical Evidence for the Structures of **12 and **13**.** The proposed structures of **12** and **13** suggested that the progenitor of these regioisomers was 2,5-bi-*S*-CyS-DA. The latter cysteinyl conjugate is a major early product of oxidations of DA in the presence of CySH. However, because of its ease of oxidation, 2,5-bi-*S*-CyS-DA is the precursor of 2,5,6-tri-*S*-CyS-DA (particularly in the presence of large molar excesses of CySH), DHBT-2 (minor product), DHBT-6 (major product) (2). The HPLC revealed that oxidations (100 mV) of 2,5-bi-*S*-CyS-DA, DHBT-2, and DHBT-6 in phosphate buffer (pH 7.4) all yield **12** (minor) and **13** (major). Furthermore, using HPLC method I, 2,5-bi-*S*-CyS-DA, DHBT-2, and DHBT-6 all eluted under the peaks at $t_R < 20$ min. These are the peaks that decrease and disappear upon oxidation of DA in the presence of CySH at 100 mV (Figure 1B) or as a result of more prolonged oxidations at lower applied potentials (data not shown). Taken together, these results indicate that 2,5-bi-*S*-CyS-DA, DHBT-2, and DHBT-6 are precursors of **12** and **13** and provide unequivocal evidence for sites of attachment of the sulfur residues in the latter compounds.

Spectroscopic Evidence for the Structures of **12 and **13**.** Based on high-accuracy FAB-MS results, both **12** and **13** had a molar mass of 309 g and molecular formula C₁₃H₁₅N₃O₂S₂. The preceding chemical evidence indicated that **12** and **13** were both formed as a result of oxidations of 2,5-bi-*S*-CyS-DA, DHBT-2, and DHBT-6. Thus, the sulfur atoms in **12** and **13** must be attached to C-1 and C-4 (corresponding to the C-2 and C-5 positions, respectively, in the original residue of DA). Furthermore, the molar masses of **12** and **13** (309 g) indicate that upon oxidation (2e, 2H⁺) both cysteinyl residues of 2,5-bi-*S*-CyS-DA and the single cysteinyl residues of both DHBT-2 and DHBT-6 must undergo intramolecular cyclization (condensation) and that loss of one carboxyl group occurs. The similarities between the UV-visible and ¹H NMR (300 MHz) spectra of **12** and **13** together with their identical molar masses and the fact that they are both formed by oxidations of 2,5-bi-*S*-CyS-DA, DHBT-2, and DHBT-6 clearly support the conclusion that these compounds are regioisomers derived from a common precursor that can decarboxylate from two different sites. Because of the low solubilities of both **12** and **13** in all common deuterated solvents (D₂O, CD₃OD, Me₂SO-*d*₆, pyridine-*d*₅), it was not possible to employ further NMR experiments to arrive at definitive structures directly using either compound. Accordingly, **12** and **13** were reduced by NaBH₄ to **14** and **15**, respectively (see Materials and Methods). The latter compounds were appreciably more soluble. Spectroscopic information on these compounds, including ¹H NMR (300 MHz) spectra, are presented in Materials and Methods. However, these spectra do not allow unequivocal structure assignments. Because of the significantly higher yields of **13**, and hence **15**, additional

NMR experiments focused on the latter compound. A summary of the ^1H NMR (500 MHz), ^{13}C (125 MHz), heteronuclear multiple-quantum coherence (HMQC), and heteronuclear multiple-bond connectivity (HMBC) NMR spectra of **15** is presented in Table 1. Homonuclear decoupling and 2D COSY experiments were consistent with coupling between the resonances assigned to $\text{C}(\alpha)\text{-H}_2$ and $\text{C}(\beta)\text{-H}_2$, $\text{C}(1')\text{-H}_2$ and $\text{C}(2')\text{-H}$, and $\text{C}(9')\text{-H}_2$ and $\text{C}(10')\text{-H}_2$ (data not shown). The following discussion of the structure determination of **15** relies mainly on long-range $^1\text{H}\text{-}^{13}\text{C}$ connectivity spectra (HMBC). To assist in the discussion, the proposed structure of **15** and atom numbering system is shown in Table 1. Starting at the most upfield protons, $\text{C}(\beta)\text{H}_2$ at 2.80 ppm (t, 2H), connectivity is observed to $\text{C}\text{-}\alpha$ (38.00 ppm), nonprotonated carbons at 131.88 (C-6) and 112.97 (C-1) ppm, and a protonated carbon (C-5) at 118.12 ppm. Connectivity between $\text{C}(\alpha)\text{H}_2$ and a nonprotonated carbon at 131.88 ppm confirms the point of attachment of the ethylamino side chain at C-6. Similarly, connectivity between $\text{C}(5)\text{H}$ (s, 6.51 ppm) and a methylene carbon at 29.68 ppm (C- β) and a nonprotonated carbon at 112.97 ppm (C-1) permits assignments of the C-1 and C-5 positions. Connectivity between two nonequivalent methylene protons at C-1' (3.03 ppm, dd; 3.25 ppm, dd) and a nonprotonated carbon at 112.97 ppm (C-1), a protonated carbon at 52.58 (C-2'), and the carboxylic acid carbonyl carbon at 174.54 ppm together establish that the carboxyl group-containing dihydrobenzothiazine residue is connected 1,2-*b* to the aromatic ring. Connectivity between the methylene protons at C-9' (3.67 ppm, m, 2H) and the methylene carbon at 22.33 ppm (C-10'), a nonprotonated carbon at 117.13 ppm (C-3) and between $\text{C}(5)\text{H}$ (6.51 ppm, 1H) and a nonprotonated carbon at 117.13 ppm (C-3) confirm that the carboxyl group-free dihydrobenzothiazine residue in **15** is connected 4,3-*b'* to the aromatic ring. The structure assigned to **15**, together with the spectroscopic information provided for its oxidized form, **13**, lead to the conclusion that the latter compound possesses a carboxyl-substituted dihydrobenzothiazine residue connected 1,2-*b* to the aromatic ring. Accordingly, the unsaturated carboxyl residue-free 1,4-benzothiazine residue in **13** must be attached 4,3-*b'* to the aromatic ring. **12**, therefore, is a regioisomer of **13** with the carboxyl residue attached at C-9' in the dihydrobenzothiazine residue attached 4,3-*b'* to the aromatic ring.

Cyclic Voltammetry of 12 and 13. Cyclic voltammograms of **12** and **13** (1.0 mM) in phosphate buffer (pH 7.4; $\mu = 1.0$) at a sweep rate of 50 mV s^{-1} are presented in Figure 2. Thus, **12** exhibits three voltammetric oxidation peaks at peak potentials (E_p) of 128, 421, and 586 mV (Figure 2A). **13** exhibits three oxidation peaks at $E_p = 155, 473, \text{ and } 596\text{ mV}$ (Figure 2B).

Preliminary Biological Experiments. **12** was dissolved in 70:30 (v/v) isotonic saline/ Me_2SO ; **13** was dissolved in isotonic saline. Solutions of each compound dissolved in $5\text{ }\mu\text{L}$ of vehicle were injected into the vicinity of the left lateral ventricle while mice were maintained under ether anesthetic (see Materials and Methods for procedures employed). The LD_{50} values, used as a measure of toxicity and defined as the dose of injected compound (expressed as free base) at which 50% of treated animals died, were determined using the statistical method of Dixon (24) in order to minimize the number of animals needed (~ 25). All animals that died did so at times of $\leq 1\text{ h}$ after administration of **12** or **13**. Because BT-1 could not be isolated in a pure form, biological

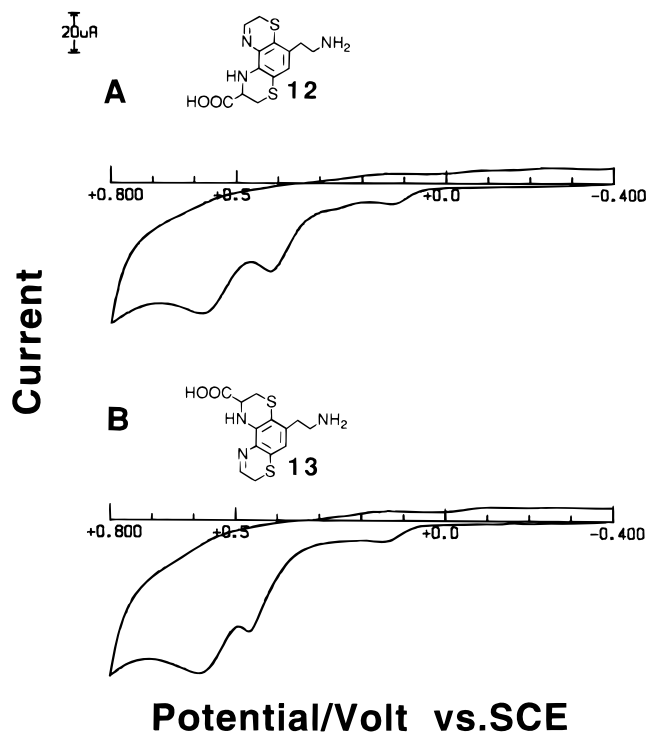


Figure 2. Cyclic voltammograms at the PGE of 1.0 mM solutions of (A) **12** and (B) **13** in phosphate buffer (pH 7.4; $\mu = 1.0$) at a sweep rate of 50 mV s^{-1} .

studies on this compound were not carried out. However, both **12** and **13** were lethal, having experimental LD_{50} values of $18.5 \pm 1.3\text{ }\mu\text{g}$ ($578 \pm 41\text{ }\mu\text{g/kg}$ of body weight) (mean \pm standard deviation) and $1.5 \pm 1.1\text{ }\mu\text{g}$ ($47 \pm 34\text{ }\mu\text{g/kg}$ of body weight), respectively. Doses of **12** ranging from 15 to $25\text{ }\mu\text{g}$, and of **13** ranging from 1 to $10\text{ }\mu\text{g}$, were employed to determine LD_{50} values. Solutions of **12** and **13** in vehicle were freshly prepared prior to administration to animals. HPLC analysis (method I) of these solutions after animal experiments were completed revealed insignificant decomposition.

The neurobehavioral responses evoked by **12** and **13** were similar to those evoked by other lethal DHBTs (1, 2). Thus, following an LD_{50} dose, animals exhibited extreme hyperactivity characterized by episodes of rapid running, jumping, and rolling along the head-tail axis that was accompanied by repetitive squeaking. Episodes of severe trembling occurred. Control animals treated with $5\text{ }\mu\text{L}$ of vehicle alone exhibited none of these neurobehavioral responses and all survived.

Discussion

Previous studies (1-3, 9) established that CySH can divert the in vitro oxidation of DA to melanin polymer (5) by scavenging *o*-quinone **1** to give principally 5-*S*-CyS-DA along with much smaller amounts of 2-*S*-CyS-DA. The facile oxidation of these cysteinyl conjugates then leads to more highly substituted cysteinyl-dopamines and DHBTs, some of which are shown in Scheme I. The results of this and earlier studies (3) together reveal that *o*-quinone imine **5**, formed by oxidation of both 5-*S*-CyS-DA and DHBT-1, rearranges (tautomerizes) to yellow BT-1 (Scheme 2). The latter 1,4-benzothiazine is a major product of oxidation of DA in the presence of CySH.

Based upon the structures and yields of products formed when DA is oxidized in the presence of free CySH at pH 7.4 it is clear that 2,5-bi-*S*-CyS-DA, formed

primarily by nucleophilic addition of CySH to *o*-quinone **2**, is a major precursor of many identified products. However, yields of 2,5-bi-*S*-CyS-DA are low at any stage of the oxidation reaction (**2**) owing to the great ease of oxidation of this conjugate. The oxidation of 2,5-bi-*S*-CyS-DA generates *o*-quinone **4** that can undergo intramolecular cyclizations to *o*-quinone imines **7** and **8** (Scheme 2) (**2**). In order to account for formation of DHBT-2 and DHBT-6 when 2,5-bi-*S*-CyS-DA is oxidized even in the absence of free CySH, it is clear that **7** and **8** can chemically oxidize this cysteinyl conjugate by the reaction pathways shown in Scheme 2 and discussed in detail elsewhere (**2**). However, the present study establishes that oxidations of 2,5-bi-*S*-CyS-DA, DHBT-2, and DHBT-6 also result in formation of the regioisomers **12** and **13**, the latter always being the major product. Accordingly, it can be concluded that intramolecular cyclizations of both cysteinyl residues of **4**, formed by oxidation (2e, 2H⁺) of 2,5-bi-*S*-CyS-DA, leads to the tricyclic *o*-diimine **11**. Decarboxylation of **11** from C-2' or C-9', the preferred route, then leads to regioisomers **12** and **13**, respectively (Scheme 2). Borohydride reduction of **12** and **13** to **14** and **15**, respectively, provides a valuable method to convert these sparingly soluble benzothiazines into much more soluble dihydrobenzothiazines. Spectroscopic evidence, particularly on **15**, permits unequivocal structure assignment and hence the structure of **13**. The bright yellow color that progressively develops during oxidations of DA in the presence of CySH can be traced primarily to BT-1, **12**, and **13**, i.e., products derived 5-*S*-CyS-DA and from 2,5-bi-*S*-CyS-DA, DHBT-2, and DHBT-6, respectively.

The upregulation of nigral γ -GT (**10**), irreversible loss of GSH (**18–20**), and increased 5-*S*-CyS-DA/DA concentration ratio (**21**) are all compatible with the hypothesis that an elevated translocation of CySH into neuromelanin-pigmented SN neurons might occur in PD. The observation that surviving dopaminergic cells are less heavily pigmented in the Parkinsonian SN compared to age-matched controls (**15–17**) would also be expected, by analogy with the results of in vitro studies, as a consequence of the diversion of the neuromelanin pathway by CySH. The in vitro products of oxidation of DA in the presence of free CySH include not only 5-*S*-CyS-DA but, as a consequence of the fact that this conjugate is more easily oxidized than the neurotransmitter (**1**, **2**), many additional cysteinyl dopamines, DHBTs, BT-1, **12**, and **13**. Whether a similarly complex mixture of metabolites is formed in the cytoplasm of neuromelanin-pigmented SN neurons in PD remains to be established. However, that the initial step in formation of such metabolites occurs in PD is supported by the increased 5-*S*-CyS-DA/DA ratio in the SN (**21**) and the increased 5-*S*-CyS-DA/HVA ratio in CSF (**22**). Furthermore, a number of lines of evidence support the conclusion that 5-*S*-CyS-DA is formed as a result of oxidation of cytoplasmic DA (**21**, **25**, **26**). Particularly in the cytoplasm of pigmented SN neurons, in which DA is autoxidized to form neuromelanin (**6**, **7**), 5-*S*-CyS-DA must almost certainly undergo further oxidation. In the presence of free CySH such an in vivo oxidation reaction would lead to the more complex cysteinyl dopamines, DHBTs, BT-1, **12**, and **13** that are formed in the in vitro reaction. The results presented in this and earlier reports (**1**, **2**) indicate that 2,5-bi-*S*-CyS-DA, DHBT-1, DHBT-2, DHBT-5, DHBT-6 (and other DHBTs), **12**, and **13** are toxic (lethal) when administered into the ventricular system of mice and evoke a charac-

teristic neurobehavioral response. Interestingly, **13** (LD₅₀ = 1.5 μ g), the major product of oxidation of 2,5-bi-*S*-CyS-DA (LD₅₀ = 37 μ g), DHBT-2 (LD₅₀ = 70 μ g), and DHBT-6 (LD₅₀ = 17 μ g), is the most toxic compound discovered in these investigations. Thus, it appears that as the oxidation reactions of DA in the presence of CySH progress through cysteinyl dopamines and DHBTs to **13** increasingly toxic putative metabolites are formed. These observations raise the possibility that one or more of these putative nigral metabolites might be endotoxins that contribute to SN cell death in PD. However, there is currently no evidence that any of these compounds are dopaminergic neurotoxins or that they are formed in the Parkinsonian brain. Nevertheless, all other factors being equal, intraneuronal formation of 5-*S*-CyS-DA, other cysteinyl dopamines, DHBTs, BT-1, **12**, and **13** would be expected to be most extensive in those neurons that sustain the highest basal levels of DA autoxidation, i.e., SN cells normally most heavily pigmented with neuromelanin. Thus, it may be significant that such neurons appear to be preferentially vulnerable to degeneration in PD (**15–17**).

In summary, three new compounds, BT-1, **12**, and **13**, have been identified as products formed in the relatively late stages of the in vitro oxidation of DA in the presence of CySH. The immediate precursor of BT-1 is DHBT-1. The immediate precursors of **12** and **13** are 2,5-bi-*S*-CyS-DA, DHBT-2, and DHBT-6. The results presented and hypothesis advanced in this paper are based on the influence of CySH on the in vitro electrochemically driven oxidation of DA, the toxicity of many resulting products, and other known changes that are known to occur in the Parkinsonian brain. While it is plausible to expect that similar chemistry would accompany the autoxidation of DA in pigmented dopaminergic SN cells as a result of the hypothesized γ -GT-mediated translocation of CySH into these neurons, this remains to be experimentally verified. Furthermore, while a rather remarkable number of products formed from the electrochemical oxidation of DA in the presence of CySH are relatively potent toxins in mouse brains, particularly **13**, it must be emphasized that it is not yet known whether any of these putative nigral metabolites evoke degeneration of SN neurons and therefore might play a role in the pathogenesis of PD.

Acknowledgment. This work was supported by Grant NS-29886 from the National Institutes of Health.

References

- (1) Zhang, F., and Dryhurst, G. (1994) Effects of L-cysteine on the oxidation chemistry of dopamine: New reaction pathways of potential relevance to idiopathic Parkinson's Disease. *J. Med. Chem.* **37**, 1084–1098.
- (2) Shen, X.-M., and Dryhurst, G. (1996) Further insights into the influence of L-cysteine on the oxidation chemistry of dopamine: Reaction pathways of potential relevance to Parkinson's Disease. *Chem. Res. Toxicol.* **9**, 751–763.
- (3) Zhang, F., and Dryhurst, G. (1995) Reactions of cysteine and cysteine derivatives with dopamine-*o*-quinone and further insights into the oxidation chemistry of 5-*S*-cysteinyl dopamine: Potential relevance to idiopathic Parkinson's Disease. *Bioorg. Chem.* **23**, 193–216.
- (4) Tse, D. C. S., McCreery, R. L., and Adams, R. N. (1976) Potential oxidative pathways of brain catecholamines. *J. Med. Chem.* **19**, 37–40.
- (5) Zhang, F., and Dryhurst, G. (1993) Oxidation chemistry of dopamine: Possible insights into the age-dependent loss of dopaminergic nigrostriatal neurons. *Bioorg. Chem.* **21**, 392–410.
- (6) Graham, D. G. (1978) Oxidation pathways for catecholamines in the genesis of neuromelanin and cytotoxic quinones. *Mol. Pharmacol.* **14**, 633–643.

- (7) Rodgers, A. D., and Curzon, G. (1975) Melanin formation by human brain in vitro. *J. Neurochem.* **24**, 1123–1129.
- (8) Slivka, A., Mytilineou, C., and Cohen, G. (1987) Histochemical evaluation of glutathione in brain. *Brain Res.* **409**, 275–284.
- (9) Carstam, R., Brinck, C., Hindemith-Augustsson, A., Rorsman, H., and Rosengren, E. (1991) The neuromelanin of the human substantia nigra. *Biochim. Biophys. Acta* **1097**, 152–160.
- (10) Sian, J., Dexter, D. T., Lees, A. J., Daniel, S., Jenner, P., and Marsden, C. D. (1993) Glutathione-related enzymes in brain in basal ganglia degenerative disorders. *Ann. Neurol.* **36**, 356–361.
- (11) Orłowski, M., and Meister, A. (1979) The γ -glutamyl cycle. A possible transport system for amino acids. *Proc. Natl. Acad. Sci. U.S.A.* **67**, 1248–1255.
- (12) Meister, A. (1974) Glutathione: Metabolism and function via the γ -glutamyl cycle. *Life Sci.* **15**, 177–190.
- (13) Raps, S. P., Lai, J. C. K., Hertz, L., and Cooper, A. J. L. (1989) Glutathione is present in high concentrations in cultured astrocytes but not in cultured neurons. *Brain Res.* **493**, 398–401.
- (14) Sagara, J.-L., Miura, K., and Bannai, S. (1993) Maintenance of neuronal glutathione by glial cells. *J. Neurochem.* **61**, 1672–1676.
- (15) Mann, D. M. A., and Yates, P. O. (1983) Possible role of neuromelanin in the pathogenesis of Parkinson's disease. *Mech. Ageing Dev.* **21**, 193–203.
- (16) Hirsch, E. C., Graybiel, A. M., and Agid, Y. (1988) Melanized dopaminergic neurons are differentially susceptible to degeneration in Parkinson's Disease. *Nature* **334**, 345–348.
- (17) Kastner, A., Hirsch, E. C., Lejeune, O., Javoy-Agid, F., Roscol, O., and Agid, Y. (1992) Is the vulnerability of neurons in the substantia nigra of patients with Parkinson's Disease related to their neuromelanin content? *J. Neurochem.* **59**, 1080–1089.
- (18) Jenner, P., Dexter, D. T., Sian, J., Schapira, A. H. V., and Marsden, C. D. (1992) Oxidative stress as a cause of nigral cell death in Parkinson's Disease and Incidental Lewy Body Disease. *Ann. Neurol.* **32** (Suppl.), S82–S87.
- (19) Riederer, P., Sofic, E., Rausch, W. D., Schmidt, B., Reynolds, G., Jellinger, K., and Youdim, M. B. H. (1989) Transition metals, ferritin, glutathione and ascorbic acid in Parkinsonian brain. *J. Neurochem.* **52**, 515–520.
- (20) Dexter, D. T., Sian, J., Jenner, P., and Marsden, C. D. (1993) Implications of alterations in trace element levels in brain in Parkinson's Disease and other neurological disorders affecting the basal ganglia. *Adv. Neurol.* **60**, 273–281.
- (21) Fornstedt, B., Brun, A., Rosengren, E., and Carlsson, A. (1989) The apparent autooxidation rate of catechols in dopamine-rich regions of human brains increases with the degree of depigmentation of substantia nigra. *J. Neural. Transm.* **1** (P-D Sect.), 279–295.
- (22) Cheng, F.-C., Kuo, J.-S., Chia, L.-G., and Dryhurst, G. (1996) Elevated 5-S-cysteinyl-dopamine/homovanillic acid ratio and reduced homovanillic acid in cerebrospinal fluid: Possible markers for and potential insights into the pathoetiology of Parkinson's Disease. *J. Neural Transm.* **103**, 433–446.
- (23) Napolitano, A., Costantini, C., Crescenzi, O., and Protà, G. (1994) Characterization of 1,4-benzothiazine intermediates in the oxidative conversion of 5-S-cysteinyl-dopa to pheomelanins. *Tetrahedron Lett.* **35**, 6365–6368.
- (24) Dixon, W. J. (1965) The up-and-down method for small samples. *J. Am. Stat. Assoc.* **60**, 967–978.
- (25) Fornstedt, B., and Carlsson, A. (1989) A marked rise in 5-S-cysteinyl-dopamine levels in guinea-pig striatum following reserpine treatment. *J. Neural Transm.* **76**, 155–161.
- (26) Carlsson, A. (1991) Role of brain monoamines and other neurotransmitters in normal and pathological aging. In *Alzheimer's and Parkinson's Disease II: Basic and Therapeutic Strategies* (Nagatsu, T., Iishee, A., and Yoshida, M., Eds.) Elsevier, New York.

TX960145C